

Geometric Entanglement in Valance-Bond-Solid state

H. T. Cui, C. M. Wang and S. Z. Yuan

School of Physics and Electronic Engineering, Anyang Normal University, Anyang 455000, China e-mail: cuiht@aynu.edu.cn

Received: / Revised version: October 30, 2018

Abstract. Multipartite entanglement, measured by the geometric entanglement(GE), is discussed for integer spin Valance-Bond-Solid (VBS) state respectively with periodic boundary condition(PBC) and open boundary condition(OBC) in this paper. The optimization in the definition of geometric entanglement can be reduced greatly by exploring the symmetry of VBS state, and then the fully separable state can be determined explicitly. Numerical evaluation for GE by the random simulation is also implemented in order to demonstrate the validity of the reductions. Our calculations show that GE is saturated by a finite value with the increment of particle number, that means that the total entanglement for VBS state would be divergent under the thermodynamic limit. Moreover it is found that the scaling behavior of GE with spin number s is fitted as $\alpha \log(s + \frac{\beta}{s} + \gamma) + \delta$, in which the values of the parameters $\alpha, \beta, \gamma, \delta$ are only dependent on the parity of spin s . A comparison with entanglement entropy of VBS state is also made, in order to demonstrate the essential differences between multipartite and bipartite entanglement in this model.

PACS. 75.10.Pq Spin chain models; 03.67.Mn Entanglement production, characterization and manipulation; 03.65.Ud Entanglement and quantum nonlocality

1 Introduction

The crossover between quantum information and statistical mechanics fertilizes a distinct insight into the many-body effects and intrigues extensive interests [1, 2]. Especially inspired by the pioneer works by Osterloh, *et.al.* [3] and Osborne and Nielsen [4], quantum entanglement in many-body systems has received great attention, especially on the critical systems [1, 5]. This interest can be attributed to the following points. It is well known that the general properties of critical systems can be obtained by identifying the scaling behavior of the singularity for correlation functions, e.g. the correlation lengths and related critical exponents. Furthermore the vanishing of energy gap between the ground state and the first exciting state may lead to the long-range correlation even for infinitely separated particles at zero temperature. Thus it is conjectured that quantum entanglement, a special quantum correlation, could also display likewise behaviors at critical points. Some important progresses have been made in this direction. The recent studies for the block entanglement entropy have displayed the logarithmical divergency with the block size at critical points, and the universal area law has also been constructed exactly in one-dimensional spin-chain systems (see Ref. [5] and references therein). Furthermore the multipartite entanglement in many-body systems has also been shown to be maximal or to display sharp changes closed to the critical points [6–8].

From the point of quantum information, the long-range correlation implies that a stable quantum channel could be constructed easily for the transfer of quantum information [10]. For half-odd-integer antiferromagnetic Heisenberg spin systems, Lieb-Schultz-Mattis(LSM) theorem [12] states that there is no energy gap between the ground state and the first excited state under thermodynamical limit, and the long-range order exists for any finite amount of anisotropy couplings. Then the long-distance quantum teleportation can be implemented in this system [10, 11]. However the situation is different for integer spin-chain systems. Haldane’s conjecture claims that there would be a finite excitation gap above the ground state for integer-spin antiferromagnetic Heisenberg chains, and then two-point correlation decays exponentially with the distance between two particles [13]. In order to verify this interesting issue, Affleck-Kennedy-Lieb-Tasaki(AKLT) model was constructed, whose ground state is the so called valence-bond-solid(VBS) state [14]. And the two-point correlation functions for VBS state has been shown to decay exponentially because of the advent of the energy gap above the ground state [15]. Consequently it is conjectured that quantum entanglement would be absent between two long distance separated particles in AKLT model. But the fact beats all. Verstraete, *et.al.*, demonstrate that the maximal entanglement between two infinitely separated particles can be founded even in the AKLT model by only imposing local operations on the rest of the particles [16]. This finding enforces the reconsideration of the connection between quantum entanglement and correlation in many-body systems [17, 18].

Although the absence of long-range correlation in AKLT model, den Nijs and Rommelse demonstrate that a hidden antiferromagnetic order still exists, defined by a nonlocal string order parameter(SOP) [19]. This nonvanishing SOP was then shown to be related to the breakdown of hidden $Z_2 \times Z_2$ topological symmetry in AKLT model [20]. Furthermore Venuti verifies the connection between the localized entanglement and SOP for spin-1 VBS state [18]. For higher integer-spin VBS state, several generalizations of SOP have been proposed to characterize the hidden topological symmetry [21–23].

Since it is well accepted that the local operation and classical communication(LOCC) cannot increase entanglement [24], the appearance of maximal localized entanglement in AKLT model thus means that quantum entanglement is predominant in VBS state. With respect of this point, the bipartite entanglement for VBS state has been first discussed [25, 26], where the block entanglement entropy is found to be saturated as $2 \ln(s + 1)$ for spin- s VBS state. Unfortunately the behavior of entanglement entropy cannot present a clear explanation for the appearance of maximal localized entanglement in VBS state. Moreover the block entanglement entropy is insensible to the degeneracy induced by the topological symmetry. Furthermore the dependency on the parity of spin number s is absent for the entanglement entropy of VBS state, which has been manifested clearly by SOP [22]. In our point this defect could attribute to the fact that the overall information, embedded in many-body systems, is inevitably lost due to the trace-out of the superfluous degrees of freedom for obtaining the reduced density matrix. And hence bipartite entanglement seems have limited ability of the complete characterization of VBS state.

With these points the multipartite entanglement of VBS state is discussed in this paper in order to obtain the overall information embedded in VBS state. As shown in this paper, some distinguished features for VBS state can be obtained from the evaluation of multipartite entanglement, and moreover the multipartite entanglement of VBS state demonstrates different asymptotic behaviors from entanglement entropy. The paper is organized as the following. In Sec.2, geometric entanglement(GE) is introduced for the measure of multipartite entanglement. And Valence-Bond-Solid state is defined with different boundary conditions in Sec.3. In Sec.4, the main part of this paper, we present a detailed evaluation of GE. Finally the conclusions and further discussion are presented in Sec.5.

2 Geometric Entanglement

Geometric entanglement(GE) is used to measure the multipartite entanglement in this paper, which is first introduced by Shimony for bipartite pure state [27] and generalized to the multipartite case by Carteret *et.al.* [28], Barnum and

Linden [29], Wei and Goldbart [30], to the mixed state by Cao and Wang [31]. Geometric entanglement is a genuine multipartite entanglement measurement. The main idea of GE is to minimize the distance D between the entangled state $|\Psi\rangle$ and the fully separable state $|\Phi\rangle$ in the Hilbert space,

$$D = \min_{\{|\Phi\rangle\}} \{ \|\Psi\rangle - |\Phi\rangle \|^2 \}. \quad (1)$$

Given the normalized $|\Psi\rangle$ and $|\Phi\rangle$, the evaluation of D is reduced to find the maximal overlap [30]

$$A(\Psi) = \max_{\{|\Phi\rangle\}} |\langle\Phi|\Psi\rangle|. \quad (2)$$

Geometrically $A(|\Psi\rangle)$ depicts the overlap angle between the vectors $|\Psi\rangle$ and $|\Phi\rangle$ in Hilbert space. Then the larger $A(|\Psi\rangle)$ is, the shorter is the distance and the less entangled is $|\Psi\rangle$. In order to measure the entanglement in many-body systems, in this paper we adopt the definition in Ref. [8]

$$\varepsilon = \lim_{L \rightarrow \infty} -\frac{\log_2 A^2(\Psi)}{L}, \quad (3)$$

where L denotes the chain length. Eq.(3) actually defines the average entanglement per particle, and is also entanglement monotone.

With this definition, the calculation for $A(|\Psi\rangle)$ is generally difficult since the optimization. Recently two works prove independently that for the permutationally invariant entangled pure state the maximization can be attained *necessarily* by choosing a permutationally invariant pure fully separable state at the same time, whose amplitudes are all non-negative in a computational basis [32]. Moreover this conclusion has been generalized to any symmetric pure multipartite entangled state as shown in Ref. [33]. This point could be understood properly by noting the fact that $|\langle\Phi|\Psi\rangle| = 1$ means that $|\Phi\rangle$ and $|\Psi\rangle$ depict the same state, and both of them have the same physical features. While, $|\langle\Phi|\Psi\rangle| = 0$ means that $|\Phi\rangle$ and $|\Psi\rangle$ have distinct physical features, and one can easily differentiate one from another by physical measurements. Thus for the purpose of maximizing $|\langle\Phi|\Psi\rangle|$, it is necessary to find the fully separated $|\Phi\rangle$ which has the same overall features to that of $|\Psi\rangle$.

Here we present a formal proof for this intuitive speculation. The start point for this proof is Cuchy-Schwartz(CS) inequality

$$|\langle v|w\rangle|^2 \leq \langle v|v\rangle\langle w|w\rangle, \quad (4)$$

where the equality occurs if and only if the two vectors $|v\rangle$ and $|w\rangle$ in Hilbert state are linearly related, i.e. $|v\rangle = c|w\rangle$ for some scalar c . It should emphasize that c is *unnecessary* a constant, and generally would contain other variables. The trivial case for the equality occurring is that $|v\rangle$ and $|w\rangle$ are the same vector aside from the normalization constants. But for more general case, it is a nontrivial task for given $|v\rangle$ to find a physically different state $|w\rangle$ in order to maximize the overlap. However the task would become apparent if one rewrites the condition for the equality as

$$|v\rangle\langle v| |w\rangle = \langle v|v\rangle |w\rangle. \quad (5)$$

This transformation implies strongly that this task is reduced to find the eigenvector for operator $|v\rangle\langle v|$. This task seems trivial in the Hilbert space specified by vector $|v\rangle$. However it becomes nontrivial for enlarged Hilbert space. Fortunately recall that if two operators are commutative, they then share the same set of the eigenvectors, and then $|w\rangle$ has same global symmetry to $|v\rangle$. Consequently this task can be reduced to find the all symmetries T for operator $|v\rangle\langle v|$. With this tricky, the optimal process in the definition of GE can be simplified greatly.

3 Valence-Bond-Solid state

Dependent on the boundary conditions, integer spin- s VBS state can be defined respectively as [22]

$$|\text{VBS}\rangle_{\text{PBC}} = \prod_{k=1}^L (a_k^\dagger b_{k+1}^\dagger - b_k^\dagger a_{k+1}^\dagger)^s |0\rangle \quad (6)$$

with periodic boundary condition(PBC) $a_{L+1}^{(\dagger)} = a_1^{(\dagger)}$, $b_{L+1}^{(\dagger)} = b_1^{(\dagger)}$, in which $a_k^{(\dagger)}$, $b_k^{(\dagger)}$ are the Schwinger boson operators, L is the chain length and $|0\rangle$ denotes the vacuum state, or

$$\begin{aligned} |\text{VBS}; p, q\rangle &= Q_{\text{left}}(a_1^\dagger, b_1^\dagger; p) \prod_{k=1}^{L-1} (a_k^\dagger b_{k+1}^\dagger - b_k^\dagger a_{k+1}^\dagger)^s \\ &Q_{\text{right}}(a_L^\dagger, b_L^\dagger; q) |0\rangle, \end{aligned} \quad (7)$$

with open boundary condition(OBC)

$$\begin{aligned} Q_{\text{left}}(a_1^\dagger, b_1^\dagger; p) &= \sqrt{{}_s C_{p-1}} (a_1^\dagger)^{s-p+1} (b_1^\dagger)^{p-1} \\ Q_{\text{right}}(a_L^\dagger, b_L^\dagger; q) &= \sqrt{{}_s C_{q-1}} (a_L^\dagger)^{q-1} (b_L^\dagger)^{s-q+1}. \end{aligned} \quad (8)$$

in which $p, q = 1, \dots, s+1$ and ${}_n C_m$ denotes the binomial function. For OBC the VBS state is $(s+1)^2$ -fold degenerate. VBS state can be rewritten as the matrix-product form [22]

$$\begin{aligned} |\text{VBS}\rangle_{\text{PBC}} &= \text{Tr}[g_1 \cdot g_2 \cdots g_L] \\ |\text{VBS}; p, q\rangle &= [g_{\text{start}} \cdot g_2 \cdots g_L]_{(p,q)} \end{aligned} \quad (9)$$

where (p, q) denote the coordinates of matrix elements, and the matrix g_i is $(s+1) \times (s+1)$ dimension, of which the element reads

$$\begin{aligned} g_i(p, q) &= (-1)^{s+p-1} \sqrt{{}_s C_{p-1} {}_s C_{q-1}} \sqrt{(s-p+q)!(s+p-q)!} |s; q-p\rangle_i \\ g_{\text{start}}(p, q) &= \sqrt{{}_s C_{p-1} {}_s C_{q-1}} \sqrt{(s-p+q)!(s+p-q)!} |s; q-p\rangle \end{aligned} \quad (10)$$

Obviously g_i is related only to the i -th spin. Manifestly VBS state with PBC is permutationally invariant, while it is not so for OBC because of the open ends.

-*Symmetry*- VBS state is the ground state of Hamiltonian

$$H_{\text{VBS}} = \sum_{i=1}^L P_{s+1}^{2s}(\mathbf{S}_i \cdot \mathbf{S}_{i+1}), \quad (11)$$

where the operator P_{s+1}^{2s} denotes to project the spins at sites i and $i+1$ into the subspace with the total spin $J = s+1, \dots, 2s$ [14,15]. Since Hamiltonian Eq.(11) is SU(2) invariant, then $[H, \prod_{i=1}^L \exp(i\pi S_i^z)] = 0$. This symmetry is also required for VBS state

$$[|\text{VBS}\rangle\langle\text{VBS}|, \prod_{i=1}^L \exp(i\pi S_i^z)] = 0, \quad (12)$$

where $|\text{VBS}\rangle$ denotes the VBS state without specifying the boundary conditions.

-*Magnetization*- For PBC, each S_i^z eigenvalue occurs with equal probability [22], and then the reduced density matrix of single spin is the unit matrix. This implies that each eigenvalue of the total $S_z = \sum_{i=1}^L S_i^z$ also occurs with equal probability, and the total magnetization $\langle S_z \rangle_{\text{VBS}}$ in this case is zero. Furthermore $\langle S_y \rangle_{\text{VBS}} = \langle S_x \rangle_{\text{VBS}} = 0$. Thus VBS state for PBC is rotationally invariant.

The situation becomes different for OBC. VBS is not necessarily rotationally invariant because of the open ends. Moreover the open ends may induce a local perturbation to the spin chain, and the hidden topological property for VBS state can be obtained from the system's responds to this local perturbation.

4 GE in VBS state

Given these properties, one can now determine the fully separable state $|\Phi\rangle = \otimes_{i=1}^L |\phi_i\rangle$, in which $|\phi_i\rangle = \sum_{m=-s}^s c_m^{(i)} |m\rangle_i$ on the basis of $\{S_z^{(i)}; |m\rangle_i\}$ and the coefficient $c_m^{(i)}$ is generally complex and dependent on the position i . With the requirement of Eq.(12), one has $[|\Phi\rangle\langle\Phi|, \prod_{i=1}^L \exp(i\pi S_z^{(i)})] = 0$. Then two different situations can be identified as

$$\begin{aligned} \exp(i\pi S_z^{(i)}) |\phi_i\rangle^p &= |\phi_i\rangle^p \\ \exp(i\pi S_z^{(i)}) |\phi_i\rangle^n &= -|\phi_i\rangle^n \end{aligned} \quad (13)$$

where

$$\begin{aligned} |\phi_i\rangle^p &= \sum_{k=-[s/2]}^{[s/2]} c_k^{(i)} |2k\rangle_i \\ |\phi_i\rangle^n &= \sum_{k=-[(s+1)/2]}^{[(s-1)/2]} c_k^{(i)} |2k+1\rangle_i \end{aligned} \quad (14)$$

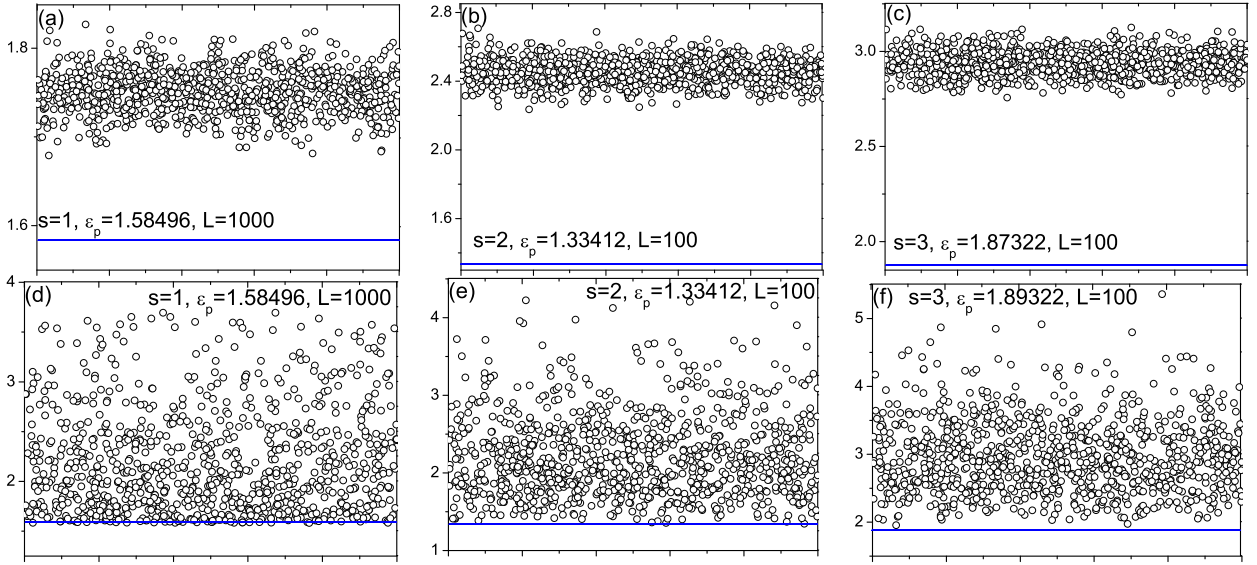


Fig. 1. (Color Online) The randomly numerical simulation of $-\frac{\log_2 |\langle \Phi | \text{VBS} \rangle|^2}{L}$ for VBS state with PBC and spin number $s = 1, 2, 3$ respectively. There is 1000 sample data for every simulation. The plots of (a), (b) and (c) correspond to the simulations without any other restriction on the coefficients $c_k^{(i)}$ of the fully separable state $|\Phi\rangle$ except of the requirement of normalization. While for plots (d), (e) and (f) the requirement of permutational invariance for $|\Phi\rangle$ has been implemented, but c_k for different k is still chosen randomly. The (blue) solid line corresponds the value of GE after applying the all approximations stated in the paper.

and $[n/2]$ denotes the maximal integer number not bigger than $n/2$. Then one has to find the maximal overlap among $\{|\langle \text{VBS} | \otimes_{i=1}^L |\phi_i\rangle^p\rangle, |\langle \text{VBS} | \otimes_{i=1}^L |\phi_i\rangle^n\rangle\}$. Consequently GE is determined by the minimization

$$\varepsilon = \min\{\varepsilon_p, \varepsilon_n\} \quad (15)$$

where $\varepsilon_{p(n)}$ denotes GE evaluated with the separable state $\otimes_{i=1}^L |\phi_i\rangle^{p(n)}$ respectively. Dependent on the boundary conditions, the following discussion has to be divided into two subsections.

4.1 Periodic Boundary Condition

As displayed in Sec.3, VBS state is permutationally invariant in this case. It has been proved in Refs. [32, 33] that the fully separable state is necessarily also permutationally invariant in order to maximize the overlap. Then the fully separable state $|\Phi\rangle$ becomes in this case

$$\begin{aligned} |\Phi\rangle_p &= (|\phi\rangle^p)^{\otimes L} \\ |\Phi\rangle_n &= (|\phi\rangle^n)^{\otimes L}. \end{aligned} \quad (16)$$

Another important feature is that VBS state is rotationally invariant for PBC, and hence has zero total spin [15]. It is natural to endow the fully separable state $|\Phi\rangle_{p(n)}$ with the same character. This point is evident to note that it belongs to completely different space for the states which has vanishing total spin or not, and then the overlap between states in the two distinct spaces must be zero.

With this requirement, the coefficient $c_k^{(i)}$ preferably has the same amplitude, independent both of the position i and quantum number k . Moreover $c_k^{(i)}$ should preferably be in phase in order to maximize the overlap with respect of the special form of VBS state shown by Eq.(6). This point becomes clear by noting first that ${}^p\langle\phi| \otimes g_i$ has a block-diagonal form dependent on the parity of p, q for any spin s (see Appendix A for more detail). Set $c_k = c_{p-q} = |c_{p-q}| e^{i\theta_{p-q}}$, of which θ_{q-p} and $|c_{p-q}|$ depend only on the difference $|q-p|$. And then

$${}^p\langle\phi| \otimes g_i = \begin{pmatrix} \boxed{|c_{p-q}| e^{i\theta_{q-p}} g_{p,q} (\text{even } p \text{ and } q)} & 0 \\ 0 & \boxed{|c_{p-q}| e^{i\theta_{q-p}} g_{p,q} (\text{odd } p \text{ and } q)} \end{pmatrix} \quad (17)$$

where the dashed boxes denote the sub-matrixes satisfying the conditions stated in the brackets, and the element of the sub-matrix is read

$$g_{p,q} = (-1)^{s+p-1} \sqrt{s C_{p-1} C_{q-1}} \sqrt{(s-p+q)!(s+p-q)!}.$$

Then one has

$$\begin{aligned} |{}_p\langle\Phi|VBS\rangle_{\text{PBC}}| &= |\text{Tr}[_p\langle\Phi|g_1 \cdot g_2 \cdots g_L]| = \left| \sum_{p_1, p_2, \dots, p_L; q_1, q_2, \dots, q_L=1}^{s+1} \prod_{i=1}^L |c_{p_i - q_i}| \prod_{i=1}^L e^{i\theta_{q_i - p_i}} g_{p_i, q_i} \right| \\ &\leq |c_p|^L \left| \sum_{p_1, p_2, \dots, p_L; q_1, q_2, \dots, q_L=1}^{s+1} \prod_{i=1}^L e^{i\theta_{q_i - p_i}} g_{p_i, q_i} \right| \\ &\leq |c_p|^L \sum_{p_1, p_2, \dots, p_L; q_1, q_2, \dots, q_L=1}^{s+1} \prod_{i=1}^L |e^{i\theta_{q_i - p_i}} g_{p_i, q_i}| \\ &= |c_p|^L \sum_{p_1, p_2, \dots, p_L; q_1, q_2, \dots, q_L=1}^{s+1} \prod_{i=1}^L |g_{p_i, q_i}|, \end{aligned} \tag{18}$$

where the following relation is used

$$\prod_{i=1}^L |c_{p_i - q_i}| \leq \frac{\sum_{i=1}^L |c_{p_i - q_i}|^L}{L}, \tag{19}$$

in which the equality occurs if and only if $|c_{p_i - q_i}| = |c_{p_j - q_j}| = |c_p|$ for arbitrary $i \neq j$.

With even L and noting the common factor $(-1)^{s+p-1}$ in $g_{p,q}$, then

$$|{}_p\langle\Phi|VBS\rangle_{\text{PBC}}| \leq |c_p|^L \sum_{p_1, p_2, \dots, p_L; q_1, q_2, \dots, q_L=1}^{s+1} \prod_{i=1}^L g_{p_i, q_i}. \tag{20}$$

which means that one need only choose c_p being non-negative real for the maximization of the overlap. As for odd L , one should note that ${}_p\langle\phi| \otimes g_i$ is traceless and the overlap always vanishes.

For $|\phi\rangle^n$, ${}_n\langle\phi| \otimes g_i$ has a block-anti-diagonal form with opposite sign for the two blocks, as shown in Appendix A, and thus the overlap always vanishes for odd L . For even L one only notes that the product of two block-anti-diagonal matrixes is block-diagonal, and the two diagonal block has the same sign after this product. Then the analysis is applicable in this case.

Then the fully separable state can be determined exactly

$$\begin{aligned} |\Phi\rangle_p &= \bigotimes_{i=1}^L c_p \sum_{k=-[s/2]}^{[s/2]} |2k\rangle_i \\ |\Phi\rangle_n &= \bigotimes_{i=1}^L c_n \sum_{k=-[(s+1)/2]}^{[(s-1)/2]} |2k+1\rangle_i \end{aligned} \tag{21}$$

in which $c_p = 1/\sqrt{1+2[s/2]}$, $c_n = 1/\sqrt{2[(s+1)/2]}$. Then with respect of the matrix-product form of VBS state, the overlap can be expressed readily as

$$\begin{aligned} \Lambda_p &= \frac{|{}_p\langle\Phi|VBS\rangle_{\text{PBC}}|}{\sqrt{\text{PBC}(VBS|VBS)_{\text{PBC}}}} = \frac{\text{Tr}[_p\langle\Phi|g_1 \cdot g_2 \cdots g_L]}{\sqrt{\text{Tr}[g_1^* \cdot g_2^* \cdots g_L^* \otimes g_1 \cdot g_2 \cdots g_L]}} \\ \Lambda_n &= \frac{|{}_n\langle\Phi|VBS\rangle_{\text{PBC}}|}{\sqrt{\text{PBC}(VBS|VBS)_{\text{PBC}}}} = \frac{\text{Tr}[_n\langle\Phi|g_1 \cdot g_2 \cdots g_L]}{\sqrt{\text{Tr}[g_1^* \cdot g_2^* \cdots g_L^* \otimes g_1 \cdot g_2 \cdots g_L]}} \end{aligned} \tag{22}$$

where g^* denotes to take Hermitian conjugate for the matrix elements, but not transpose the matrix.

In order to demonstrate more explicitly the validity of the statements above, the randomly numerical simulation has been implemented for several simple cases, as shown in Fig.1. For Fig.1(a), (b) and (c), there is no any other restriction on the choice of $c_k^{(i)}$ except of the requirement of normalization. It is obvious that the sample data are

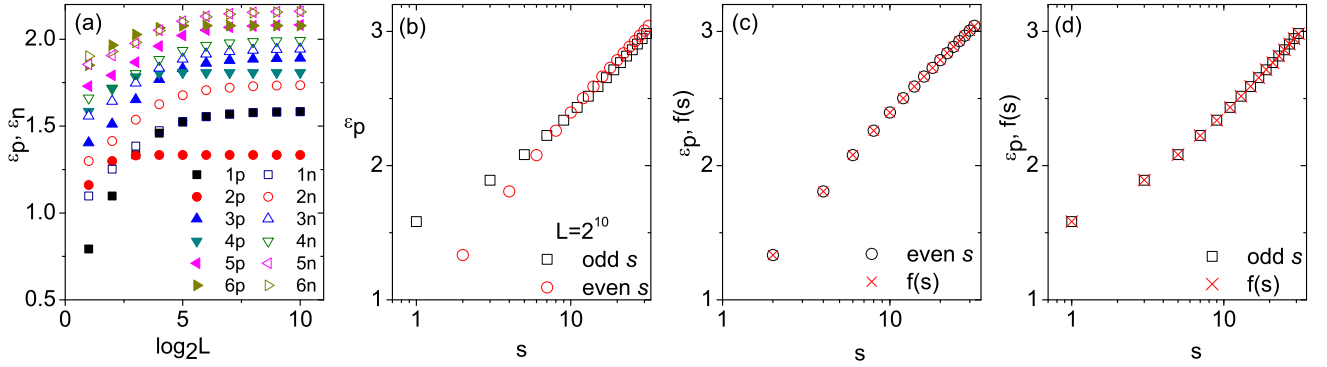


Fig. 2. (Color Online)(a) $\varepsilon_p, \varepsilon_n$ versus the particle number L with PBC. In this figure the Arab numbers denote the spin and p, n denote the plotting for $\varepsilon_p, \varepsilon_n$ respectively; (b) the scaling of ε_p with respect to spin s and the fitting function $f(s)$; Use $f(s)$ to fit GE for even(c)and odd(d) spin- s case.

Table 1. The chosen parameters for the fittings of GE in Figs.2(c) and (d).

	α	β	γ	δ
Fig. 2(c)	1.41	-0.39	2.82	0.83
Fig. 2(d)	1.15	1.67	-1.83	1.33

always bigger than the value of GE evaluated after applying the approximations. Furthermore the approximation that $c_k^{(i)}$ is a positive constant independent both of the coordinate i and quantum number k , has also been verified numerically as shown in Fig.1(d), (e) and (f). The results show that this approximation is really proper and correct. With the assistance of the numerical simulation, GE can be evaluated readily.

For arbitrary spin- s the analytical expressions for the overlap are difficult to obtain. Thus $\varepsilon_p, \varepsilon_n$ are plotted numerically in Fig. 2(a). It is obvious that $\varepsilon_p, \varepsilon_n$ tend to be saturated with the increment of particle number L . Moreover one can note $\varepsilon_p < \varepsilon_n$ under large L . As our study is implemented mainly under the limit of large L , the discussions below would focus on ε_p .

It should emphasize that since $\varepsilon_{p(n)}$ denotes the average GE per particle, the saturation for $\varepsilon_{p(n)}$ shown in Fig. 2(a) means that the globe GE E_G for VBS state, defined first in Ref. [7], should be proportional to the particle number L , and is divergent under $L \rightarrow \infty$, i.e.

$$E_G = \varepsilon_p L. \quad (23)$$

This phenomena is distinct from the entanglement entropy of VBS state, which is shown to be saturated as $2 \ln(s+1)$ because of the appearance of energy gap above the ground state [25,26]. However the divergency of E_G strongly implies that there is hidden degeneracy not captured by entanglement entropy. With the findings of the breakdown of hidden $Z_{s+1} \times Z_{s+1}$ topological symmetry [20,23], it hints that GE would be also sensible to the existence of topological phases in many-body systems. A further discussion would be presented in the final section.

Furthermore, as shown in Fig.2(b) where the scaling behavior of ε_p with spin- s is plotted, ε_p shows two different scaling behavior, dependent on even or odd spin s . This feature is consistent with the observation that one have to define different SOPs for odd or even s VBS state. A fitting function $f(s)$ can be constructed for identifying the scaling behavior of GE with spin s ,

$$f(s) = \alpha \log\left(s + \frac{\beta}{s} + \gamma\right) + \delta \quad (24)$$

in which α, β, γ and σ are tunable parameters. The chosen values of these parameters for the fittings of ε_p are listed in Table.4.1. It has been shown that the scaling behavior with spin s for entanglement entropy of VBS state [25,26] is attributed to the tendency to be unit form for the reduced block density matrix under limit $L \rightarrow \infty$ [26]. Comparably it is unclear until now for the distinct feature of GE disclosed by Eq.(24).

The differences between entanglement entropy and GE in VBS state can intuitively attribute to the trace-out of the superfluous degrees of freedom for obtaining the reduced density matrix in order to calculate the block entanglement entropy. Thus the overall information about VBS state is lost because of this trace-out. With respect of this point, it seems not enough by only sampling a portion of the system to obtain the overall information of many-body systems.

Another interesting character for this numerical evaluation is that $\varepsilon_p, \varepsilon_n$ are sensitive to the parity of particle number L . As for odd spin s case, A_p is always vanishing for odd L and then ε_p is infinity. This point can be easily verified (see Appendix A). Whereas for even spin- s our calculation shows that A_p for odd or even L tends to be consistent numerically with the increment of particle number. The similar behavior also happens for the evaluation of ε_n .

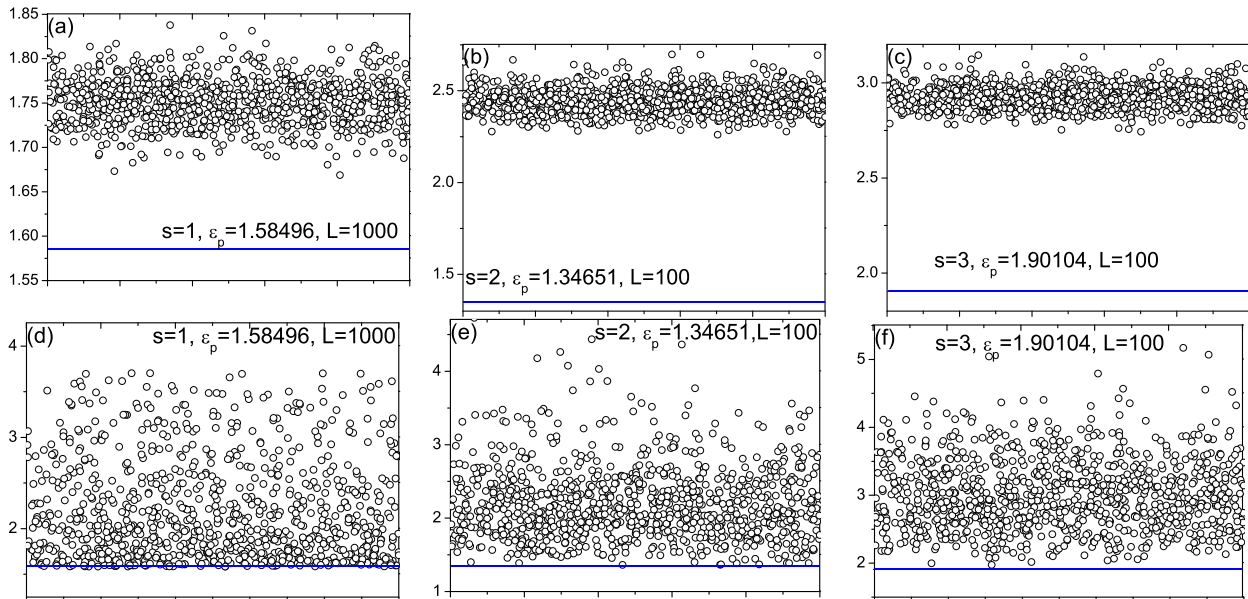


Fig. 3. (Color Online)Color Online)The randomly numerical simulation of $-\frac{\log_2 |\langle \Phi | \text{VBS} \rangle|^2}{L}$ for VBS state with OBC and spin number $s = 1, 2, 3$ respectively. There is 1000 sample data for every simulation. The plots of (a), (b) and (c) correspond to the simulations without any other restriction on the coefficients $c_k^{(i)}$ of the fully separable state $|\Phi\rangle$ except of the requirement of normalization. While for plots (d), (e) and (f) the requirement of permutational invariance for $|\Phi\rangle$ has been implemented except of the end g_{start} , but c_k for different k , including that for g_{start} , is still chosen randomly. The (blue) solid line corresponds the value of GE after applying the all approximations stated in the paper.

4.2 Open Boundary Condition

The situation becomes complex for OBC. Although the requirement Eq. (12) persists, the permutational invariance for VBS is broken in this case. Thus the assumptions made in the preceding subsection has to be reconsidered seriously.

The crucial step is still to determine the overlap $|\langle \text{VBS}; p, q | \Phi \rangle|$. It is interesting to note from the matrix-product form of $|\text{VBS}; p, q\rangle$ that except of the end g_{start} the remaining g_i s of this expression are obviously permutational invariant. With respect of the findings in Ref. [32], one could reasonably assume

$$\langle \text{VBS}; p, q | \Phi \rangle = [{}_{\text{start}} \langle \phi' | g_{\text{start}} \langle \phi | g_1 \cdots g_{L-1} \langle \phi | g_{L-1}]_{(p,q)} \quad (25)$$

Now it is crucial to find the relation between $|\phi'\rangle$ and $|\phi\rangle$.

As stated in Ref. [35], the boundary effect vanishes exponentially with increasing length of the system if one focuses on the local operator. From the definition of GE Eq.(3), it actually imposes a locally independent operator $|\phi_i\rangle\langle\phi_i|$ on the individual spin since the choice of $|\phi_i\rangle$ is independent with each other in the definition. Thus it is an acceptable approximation to ignore the effect of g_{start} on determining $|\phi'\rangle$ under the limit of large L , and let $|\phi'\rangle = |\phi\rangle$. Another important character for $g_{\text{start}} \cdot g_2 \cdots g_L$ is that the eigenvectors of single spin S_j^z occur with equal probability [22], which also means that the different boundary condition represented by (p, q) , happens with the same probability. With these observations, it also is a reasonable assumption that the coefficient $c_k^{(i)}$ could be same to that for PBC. Hence for OBC the fully separable state is same as that for PBC (see Eq. (21)).

In order to demonstrate the validity of these approximations above, the numerical simulations are implemented by randomly choosing $c_k^{(i)}$. Similar to the simulation for PBC, the plots Fig.3(a), (b) and (c) display the results of simulation without any other restriction on $c_k^{(i)}$ except of the requirement of normalization. For plots Fig.3(d), (e) and (f), the permutational invariance is imposed on the other particles except of the end g_{start} , in order to verify the approximation that $c_k^{(i)}$ is a positive constant independent of the coordinate i and quantum number k . These plots manifestly display the validity of this assumption. Furthermore the effect of OBC has been considered independently, as shown numerically in Fig.4. For this simulation, the approximations stated in the paragraph above are implemented for the particles except of the end, in order to highlight the effect of boundary condition. Obviously with the increment of particle number L , the effect of OBC tends to be vanishing. And so except for $s = 1$, this observation means that these approximations are valid even for very small L . As for $s = 1$, our further numerical simulation shows that with the increment of L , all data would become consistent with the result obtained by the approximations above. It should point out that with the consideration of the small L $\varepsilon = \varepsilon_n$, which is obviously below ε_p as shown in Fig.5. For the convenience of the comparison with previous observations, only ε_p is plotted in Fig.4(a1) and (a2).

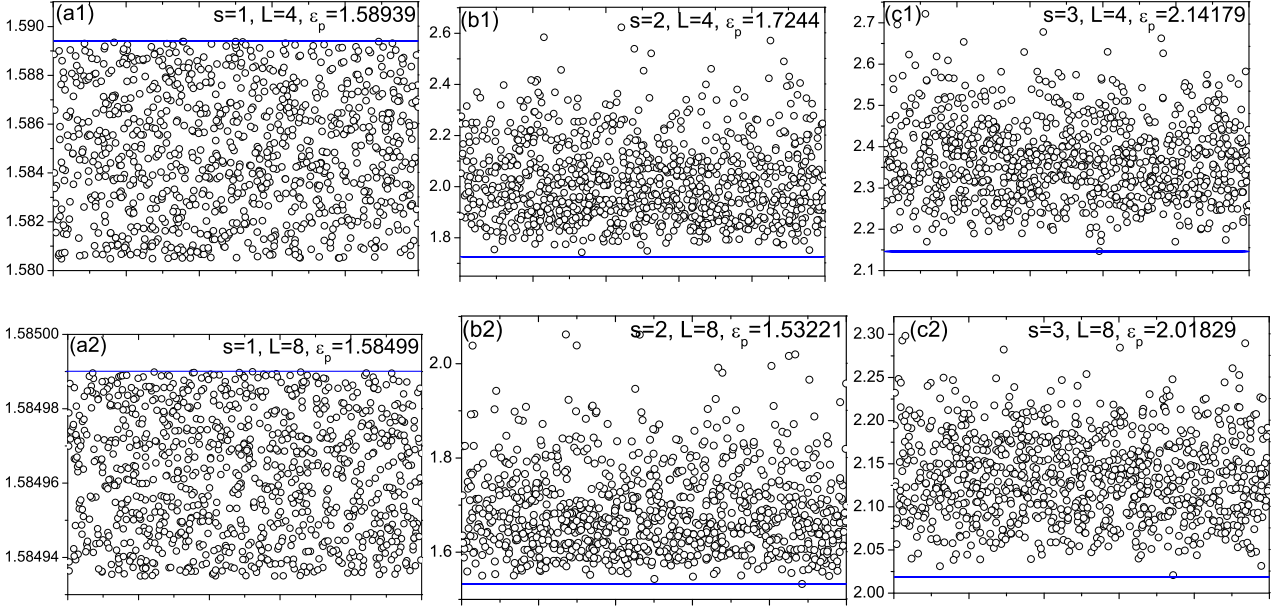


Fig. 4. (Color Online) The numerical simulations for the effect of OBC with different L . Except for the end g_{start} , the state $|\phi\rangle$ is chosen based on the approximations stated in the paper, and $|\phi\rangle_{\text{start}}$ is still randomly chosen. There is 1000 sample data for every simulation.

With these approximations, it is not difficult to find the overlap $|\langle \text{VBS}; p, q | \Phi \rangle|$. In order to eliminate the dependence on special boundary condition, the average for all degenerate states is adopted

$$|\Lambda(|\text{VBS}\rangle)|^2 = \frac{1}{(s+1)^2} \sum_{(p,q)} \frac{|\langle \text{VBS}; p, q | \Phi \rangle|^2}{\langle \text{VBS}; p, q | \text{VBS}; p, q \rangle}, \quad (26)$$

with

$$\langle \text{VBS}; p, q | \Phi \rangle^2 = [g_{\text{start}} | \phi \rangle \prod_i^{L-1} g_i | \phi \rangle_i]_{(p,q)}^2. \quad (27)$$

Since the elements of g_i and $|\phi\rangle_i$ are real, one obviously obtain under the limit of large L

$$|\Lambda(|\text{VBS}\rangle)|^2 = \frac{1}{c_L} \text{Tr}^{(2)} [g_{\text{start}} | \phi \rangle \prod_{i=1}^{L-1} g_i | \phi \rangle_i]. \quad (28)$$

where $\text{Tr}^{(2)}[M]$ denotes the sum of the square of all the elements in matrix M , and the normalization constant $c_L \approx (s+1) \left[\frac{(2s+1)!}{s+1} \right]^L$ for large L [22].

For $s=1$ one has $|\Lambda(|\text{VBS}\rangle)|^2 = 3^{-L}$ for separate states $|\Phi\rangle_p$ and $|\Phi\rangle_n$. Then we have $\varepsilon_p = \varepsilon_n = \log_2 3$ under $L \rightarrow \infty$. In a recent work of Orús [9], the author discussed the block GE for spin-1 VBS state. Our result is consistent with Orús' result when the block has only one particle. For $s=2$, $|\Lambda(|\text{VBS}\rangle)|^2 = [(4/3)^L (1+\sqrt{6})^L + (1-\sqrt{6})^L + 4^L] / c_L$ for $|\Phi\rangle_p$, and $3^L / c_L$ for separate state $|\Phi\rangle_n$. For higher s , the exact expressions for $\Lambda(|\text{VBS}\rangle)$ is difficult to find. Hence our discussion below relies on the numerical evaluation.

In Fig.5 $\varepsilon_p, \varepsilon_n$ are plotted respectively. As shown in Fig.5(a), both $\varepsilon_p, \varepsilon_n$ tend to be saturated with the increment of L , similar to the case of PBC. Moreover ε_p and ε_n are also generally unequal, as show in Fig.5(a). An intricate phenomena is that because of the finite-size effect $\varepsilon_p > \varepsilon_n$ for small L , while under the limit of large L , $\varepsilon_p < \varepsilon_n$. Comparing Fig.5 and Fig.2, our calculation show that the two ε_p are equivalent numerically under large L whether for PBC or OBC, so does for ε_n . While for small L , the value of ε_p is obviously dependent on the boundary conditions. These findings are consistent with our assumption that the boundary effects have exponentially decayed affect with the increment of system size. It means that for VBS state, geometric entanglement under thermodynamic limit is independent on the boundary condition. Hence the scaling behavior of ε_p with spin s shown in Fig. 5(b), is same to Fig.2(b) and has the same fitting functions.

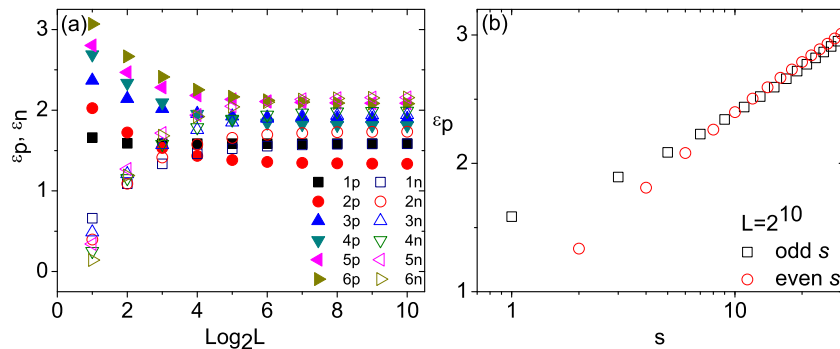


Fig. 5. (Color Online)(a) $\varepsilon_p, \varepsilon_n$ versus the particle number L with OBC. In this figure the Arab numbers denote the spin and p, n denote the plotting for $\varepsilon_p, \varepsilon_n$ respectively. (b) the scaling of ε_p with the spin s , which is very similar to Fig.2(b).

5 Conclusion and Further Discussion

In conclusion the geometric entanglement is discussed explicitly for integer spin Valence-Bond-Solid state in this paper. In order to reduce the optimization in the definition Eq.(3), we point out that the overlap between the entangled state $|\Psi\rangle$ and the fully separable state $|\Phi\rangle$ is dependent on the common symmetry shared by two states. With this important observation, the fully separable state $|\Phi\rangle$, which maximizes the overlap with VBS state, can be determined explicitly whether for PBC or OBC. For PBC, $|\Phi\rangle$ is permutational invariant and can be determined exactly. While for OBC, since the perturbation induced by the boundary condition, the fully separate state $|\Phi\rangle$ can be decided when the system size tends to be infinite, and the effect of boundary condition can be ignored in this case. Furthermore in order to display the validity of the approximations made to determine $|\Phi\rangle$ exactly, the numerical simulations have been implemented, which demonstrates clearly the validity of the approximations.

An intricate property for the evaluation of GE is that $\varepsilon_{p(n)}$ is dependent on the parity of the particle number L . The similar feature can also be found for the evaluation of entanglement entropy in one-dimensional system [36], however in which case the dependence of the parity of particle number is because of the boundary conditions. While for VBS state, the parity dependence of GE is mainly because that the elementary matrix ${}^{p(n)}\langle\phi| \otimes g_i$ is traceless. Another interesting feature for GE is that the ε_p for PBC and OBC coincides under large L . Compared to the entanglement entropy, which heavily depends on the boundary conditions [5], this feature can be considered as a manifest of the overall character of multipartite entanglement, and shows that the local boundary condition would be negligible when one focuses on the global entanglement in the system.

The important observation for GE is that ε_p becomes saturated with the increment of particle number L as shown in Fig.2(a) and Fig.5(a). Since ε_p denotes the average entanglement per particle, this feature strongly implies that the total entanglement for the whole system is proportional to the particle number L , and the globe GE E_G is divergent under $L \rightarrow \infty$. Given the appearance of the finite energy gap for the system described by the hamiltonian Eq.(11) [15], this divergency means that there is hidden symmetry for the hamiltonian Eq.11. Together with the finding of the hidden $Z_{s+1} \times Z_{s+1}$ topological symmetry for Eq.(11) [20, 23], it implies that GE could be used to detect the topological phase transition. Moreover this divergency also present a clear explanation for the appearance of maximal localized entanglement in AKLT model [16]. Since the degeneracy of ground state of Eq.(11) still exists manifested by the divergence of E_G under $L \rightarrow \infty$, it means that the long-range correlation could still be founded between any two particles. Another important observation is that the scaling behavior of ε_p with spin number s is obviously dependent on the parity of spin s shown in Fig.2(b) and Fig.5(b). This feature is consistent with the observation that different SOPs have to be chosen for odd and even spin- s VBS state in order to identify the different topological symmetries [22].

Given these points it is believed that GE could include more information of VBS state than that of entanglement entropy. These critical differences between GE and entanglement entropy for VBS state suggest that multipartite entanglement would be more popular for our understanding of the many-body effects since GE presents an overall description for many-body systems. Moreover it also hints that GE could be used to mark the different topological phases, of which the identification is still a difficult task. Another intricate points is that the convergence of GE is much slower than that of entanglement entropy [37]. In our own point, this feature can attribute to the long-distance correlation characterized by SOP.

Finally, it should point out that the definition and measurement of multipartite entanglement are a difficult task in general [38]. By the discussion of GE in VBS state, we should express our own point that it is efficient for the construction of a comprehensive understanding of multipartite entanglement to found its connection with the diverse physical phenomena, especially in many-body systems. Hence we wish this work may be useful for this purpose.

The author(Cui) thanks the helpful discussion with Dr. Chang-shui Yu and comments from Dr. Hong-Hao Tu. Especially we appreciate the criticisms from the scholars whose name we doesn't know during the preparation and submission of this paper. This work is supported by the Special Foundation of Theoretical Physics of NSF in China, Grant No. 10747159.

Appendix A

This point can be verified by noting

$$\text{Tr}_p[\langle\Phi|g_1 \cdot g_2 \cdots g_L] = \text{Tr}\left[\prod_{i=1}^L {}^p\langle\phi| \otimes g_i\right] \quad (29)$$

With respect of the expressions for g_i (Eq. (10)) and ${}^p_i\langle\phi|$ (Eq. (21)), the relation above can be rewritten as a block-diagonal matrix for $s = 2k - 1 (k = 1, 2, \dots, n)$

$${}^p\langle\phi| \otimes g_i = c_p \left(\begin{array}{ccc|ccc} \hline g_{1,1} & g_{1,3} & \cdots & g_{1,2k-1} & & \\ g_{3,1} & g_{3,3} & \cdots & g_{3,2k-1} & & \\ \vdots & & & \vdots & & \\ g_{2k-1,1} & g_{2k-1,3} & \cdots & g_{2k-1,2k-1} & & \\ \hline & & & & 0 & \\ & & & & g_{2k,2k} & g_{2k,2k-2} & \cdots & g_{2k-2,2} \\ & & & & g_{2k-2,2k} & g_{2k-2,2k-2} & \cdots & g_{2k-2,2} \\ & & & & \vdots & & & \vdots \\ & & & & g_{2,2k} & g_{2,2k-2} & \cdots & g_{2,2} \\ \hline & & & 0 & & & & \end{array} \right) \quad (30)$$

where

$$g_{p,q} = (-1)^{s+p-1} \sqrt{s C_{p-1} C_{q-1}} \sqrt{(s-p+q)!(s+p-q)!}.$$

The first submatrix correspondes to the case both of p and q being odd number, while the second submatrix corresponding to even p, q . Noting that ${}_{2k-1}C_{2k-2m-1} = {}_{2k-1}C_{2m+1-1}$, one conclude that the two submatrices are identical except of a negative sign. Moreover this matrix is independent of the coordinate i of particles, and then for odd L the trace of Eq. (29) is always zero.

However although the block-diagonal form still exists for even spin s , the two diagonal blocks do not have the same dimensions. The conclusion above is not correct for even s VBS state.

The analysis is similar for the evaluation ϵ_n . In this case ${}^n_i\langle\phi| \otimes g_i$ can be formulated as a block-antidiagonal matrix, i.e.

$${}^n_i\langle\phi| \otimes g_i = c_n \left(\begin{array}{ccc|ccc} \hline & & & g_{1,2} & g_{1,4} & \cdots & g_{1,2i} \\ & & & g_{3,2} & g_{3,4} & \cdots & g_{3,2i} \\ & & & \vdots & & & \vdots \\ & & & g_{2j-1,2} & g_{2j-1,4} & \cdots & g_{2j-1,2i} \\ \hline & & 0 & & & & \\ \hline g_{2,1} & g_{2,3} & \cdots & g_{2,2j-1} & & & \\ g_{4,1} & g_{4,3} & \cdots & g_{4,2j-1} & & & \\ \vdots & & & \vdots & & & \\ g_{2i,1} & g_{2i,3} & \cdots & g_{2i,2j-1} & & & \\ \hline & & & & & & 0 \end{array} \right) \quad (31)$$

where $i = [(s+1)/2], j = [s/2] + 1$ (the function $[f]$ denotes the integer part not more than f). Then for odd L $\text{Tr}\left[\prod_{i=1}^L {}^n_i\langle\phi| \otimes g_i\right]$ always is zero.

References

1. L. Amico, R. Fazio, A. Osterloh, and V. Vedral, *Rev. Mod. Phys.* **80**, 517 (2008).
2. A. Osterloh, e-print at arXiv:0810.1240[quant-ph].
3. A. Osterloh, L. Amico, G. Falci and R. Fazio, *Nature*, **416**, 608(2002)
4. T. J. Osborne and M. A. Nielsen, *Phys. Rev. A* **66**, 032110(2002).
5. J. Eisert, M. Cramer and M.B. Plenio, *Rev. Mod. Phys.* **82**, 277(2010) and available at e-print arXiv: 0808.3773.
6. O. Gühne, G. Tóth and H.J. Briegel, *New J. Phys.* **7**, 229(2005); T.R. de Oliveira, G. Rigolin, M.C. de Oliveira and E. Miranda, *Phys. Rev. Lett.* **97**, 170401(2006); H.T. Cui, *Phys. Rev. A*, **77**, 052105(2008); R. Orús, S. Dusuel, J. Vidal, *Phys.Rev.Lett.***100**, 130502(2008); Q.-Q. Shi, R. Orús, J. Ove Fjaerestad, H.-Q. Zhou, *New J.Phys.* **12**, 025008(2010); R. Orús, T.-C. Wei, arXiv:0910.2488v2 [cond-mat.str-el]; C.-Y. Huang and F.-L. Lin, *Phys. Rev. A* **81**, 032304 (2010); H.T. Cui, arXiv:1002.2139v3[quant-ph], accepted by PRA.
7. R. Orús, S. Dusuel, J. Vidal, *Phys. Rev. Lett.* **101**, 025701 (2008).
8. T.C. Wei, D. Das, S. Mukhopadyay, S. Vishveshwara, and P.M. Goldbart, *Phys. Rev. A* **71**, 060305(2005).
9. R. Orús, *Phys. Rev. A* **78**, 062332 (2008).
10. S. Bose, *Phys. Rev. Lett.* **91**, 207901 (2003).
11. S.M. Giampaolo and F. Illuminati, *Phys. Rev. A* **80**, 050301(R) (2009)
12. E. Lieb, T. Schultz, D. Mattis, *Ann. Phys.* **16** 407(1961); I. Affleck and E.H. Lieb, *Lett. Maht. Phys.* **12**, 57(1986).
13. F.D.M. Haldane, *Phys. Lett. A* **93**, 464(1983); *Phys. Rev. Lett.* **50**, 799(1987).
14. I. Affleck, T. Kennedy, E.H. Lieb, and H. Tasaki, *Phys. Rev. Lett.* **59**, 799(1987); *Commun. Math. Phys.* **115**, 477(1988).
15. D.P. Arovas, A. Auerach, and F.D.M. Haldance, *Phys. Rev. Lett.* **60**, 531(1988).
16. F. Verstraete, M.A. Martín-Delgado, and J.I. Cirac, *Phys. Rev. Lett.* **92**, 087201(2004).
17. L. Campos Venuti, C.D.E. Boschi, and M. Roncaglia, *Phys. Rev. Lett.* **96**, 247206 (2006).
18. L. Campos Venuti and M. Roncaglia, *Phys. Rev. Lett.* **94**, 207207(2005).
19. M. den Nijs and K. Rommels, *Phys. Rev. B* **40**, 4709(1989).
20. T. Kennedy and H. Tasaki, *Commun. Math. Phys.* **147**, 431(1992).
21. M. Oshikawa, *J. Phys.: Condens. Matter*, **4**, 7496(1992).
22. K. Totsuka and M. Suzuki, *J. Phys. A: Math. Gen.* **27**, 6443(1994); *J. Phys.: Condens. Matter*, **7**, 1639(1995).
23. H.H. Tu, G.M. Zhang, and T. Xiang, *J. Phys. A: Math. Theor.* **42** (2009) 2852.
24. G. Vidal, *J. Mod. Opt.* **47**, 355(2000).
25. H. Fan, V. Korepin, and V. Roychowdhury, *Phys. Rev. Lett.* **92**, 027901(2004); H. Fan, V. Korepin, and V. Roychowdhury, C. Halday, and S. Bose, *Phys. Rev. B* **76**, 014428(2007).
26. H. Katsura, T. Hirano, and Y. Hatsugai, *Phys. Rev. B* **76**, 012401(2007); H. Katsura, T. Hirano, and V.E. Korepin, *J. Phys. A: Math. Gen.* **41**, 135304(2008); Y. Xu, H. Katsura, and V.E. Korepin, *J. Stat. Phys.* **133**, 347-377(2008).
27. A. Shimony, *Ann. NY. Acad. Sci.*, **755**, 675(1995).
28. H. A. Carteret, A. Higureh and A. Sudbery, *J. Math. Phys.* **41**, 7932-7939(2000).
29. H. Barnum and N. Linden, *J. Phys. A: Math. Gen.* **34**, 6787(2001).
30. T.C. Wei and P.M. Goldbat, *Phys. Rev. A* **68**, 042307(2003).
31. Y. Cao and A.M. Wang, *J. Phys. A: math. and Theo.* **40**, 3507(2007).
32. Tzu-Chieh Wei and S. Severini, e-print at arXiv: 0905.0012; M. Hayashi, D. Markham, M. Muraio, M. Owari and S. Virmani, *J. Math. Phys.* **50**, 122104 (2009).
33. R. Hübener, M. Kleinmann, T.C. Wei, O. Gühne, *Phys. Rev. A* **80**, 032324 (2009) or e-print at arXiv: 0905.4822.
34. F. T. Hioe and J. H. Eberly, *Phys. Rev. Lett.* **47**, 838(1981).
35. W.D. Freitag and E. Müller-Hartmann, *Z. Phys. B-Condensed Matter*, **83**, 381(1991).
36. N. Laflorencie, Erik S. Sørensen, M.S. Chang and I. Affleck, *Phys. Rev. Lett.* **96**, 100603(2006).
37. H. Katsura, T. Hirano and Y. Hatsugai, *Phys. Rev. B* **76**, 012401 (2007).
38. C.H. Bennett, A.Grudka, M. Horodecki, P. Horodecki, and R. Horodecki, arXiv:0805.3060v2 [quant-ph](2010).